Inorg. Chem. **2002**, *41*, 4337–4347

Lead(II) Complexes with Macrocyclic Receptors Derived from 4,13-Diaza-18-crown-6

David Esteban,[†] Fernando Avecilla,[†] Carlos Platas-Iglesias,[†] Jose Mahía,[‡] Andrés de Blas,*[,†] and Teresa Rodríguez-Blas*[,†]

Departamento de Química Fundamental, Universidade da Coruña, Campus da Zapateira s/n 15071 A Coruña, Spain, and Servicios Xerais de Apoio á Investigación, Universidade da Coruña, Spain

Received January 18, 2002

The complexation properties of three related macrocycles derived from 4,13-diaza-18-crown-6 toward lead(II) are reported. The flexible macrocycle *N*,*N*′-bis(2-aminobenzyl)-4,13-diaza-18-crown-6 (**L²**) forms stable complexes with this metal ion in the presence of different counterions (perchlorate and thiocyanate). The X-ray crystal structure of $[PbL^2](SCN)_2$ indicates that, in the solid state, the lead(II) ion is eight-coordinated and fits quite well into the crown hole favoring an anti arrangement of the organic receptor, which generates a very infrequent cubic coordination polyhedron around the Pb(II) ion. In solution both complexes are fluxional and the nature of the counterion seems to affect the dynamic behavior. Ligand **L³**, *N*,*N*′-bis[(2-salicylaldimino)benzyl]-4,13-diaza-18-crown-6, derives from **L²** by condensation of salicylaldehyde with the amine group of each side arm. It can be deprotonated to yield cationic complexes of formula $[Pb(L^3\text{-}H)]^+$ where the metal ion lies asymmetrically on the cavity of the ligand, being seven-coordinated and pushed out from the crown hole, the bibracchial lariat ether presents a syn arrangement, and one of the arms remains uncoordinated. The lead(II) ion also lies asymmetrically on the cavity of the third macrocycle (**L⁷**), a lateral macrobicycle incorporating a phenolyl Schiff-base spacer. Spectrophotometric titrations of **L²** and $(L^3\text{-}2H)^{2-}$ with lead(II) perchlorate in acetonitrile gave values of log $K[PbL^2] = 7.7(5)$ and log $K[Pb(L^3\text{-}2H)] = 7.2(3)$, demonstrating that the stability of the lead(II) complexes with these two ligands is very similar.

Introduction

The coordination chemistry of macrocyclic ligands is a fascinating area of intense study for inorganic chemists. The possibility to tailor-make different types of macrocycles for specific uses has promoted much of this interest. Among others, these uses include models for biological systems, therapeutic reagents for the treatment of metal intoxication, synthetic ionophores, and the selective extraction of heavy and precious metals.[1−4]

Lead is an environmental pollutant with severe toxic effects, such as neurological and/or hematological effects.[5,6] The design of drugs to counteract the effects of lead poisoning requires establishing the preferred ligands of lead and their stereochemistry. This caused a resurgence of interest in the coordination chemistry of Pb(II),[7] and in recent years numerous reports concerning coordination chemistry of lead(II) with chelating ligands,[8] macrocycles,[9,10] lariat ethers,[11,12] and cryptands[13] have been published. In particular, we are

* Corresponding authors. E-mail: mayter@udc.es.
[†] Departamento de Química Fundamental.
[‡] Servicios Xerais de Apoio a Investigación.

(1) Izatt, R. M., Christensen, J. J., Eds. *Synthesis of Selective Agents* (*Progress in Macrocyclic Chemistry*); J. Wiley: New York, 1987.
(2) Inoue, Y., Gokel, G. W., Eds. *Cation Binding by Macrocycles*; Marcel Dekker: New York, 1990. Gokel, G. W. *Crown Ethers and Cryptands*; The Royal Society of Chemistry: Cambridge, 1991.
(3) Guerriero, P.; Tamburini, S.; Vigato, P. A. *Coord. Chem. Rev.* **1995**, *139*, 17.
(4) Yordanov, A. T.; Roundhill, D. M. *Coord. Chem. Rev.* **1998**, *170*, 93.
(5) Goyer, R. A. In *Handbook on Toxicity of Inorganic Compounds*; Seiler, H. G., Sigel, H., Sigel, A., Eds.; Marcel Dekker: New York, 1988.
(6) Jaffe, E. K.; Volin, M.; Mayers, C. B. *Biochemistry* **1994**, *33*, 11554.
(7) Parr, J. *Polyhedron* **1997**, *16*, 551.
(8) Harrowfield, J. M.; Miyamae, H.; Skelton, B. W.; Soudi, A. A.; White, A. H. *Aust. J. Chem.* **1996**, *49*, 1067.
(9) Star, A.; Goldberg, I.; Fuchs, B. *Angew. Chem., Int. Ed.* **2000**, *39*, 2685−2689.
(10) Arranz, P.; Bazzicalupi, C.; Bencini, A.; Bianchi, A.; Ciattini, S.; Fornasari, P.; Giorgi, C.; Valtancoli, B. *Inorg. Chem.* **2001**, *40*, 6383 and references therein.
(11) Damu, K. V.; Hancock, R. D.; Wade, P. W.; Boeyens, J. C. A.; Billing, D. G.; Dobson, S. M. *J. Chem. Soc., Dalton Trans.* **1991**, 293.

10.1021/ic0255095 CCC: $22.00
Published on Web 08/02/2002

Table 1. Crystal Data and Structure Refinement for $\mathbf{L^2}$, **2b**, **3b** and **5b**

	$\mathbf{L^2}$	**2b**	**3b**	**5b**
formula	$C_{26}H_{40}N_4O_4$	$C_{28}H_{40}N_6O_4PbS_2$	$C_{40}H_{50}ClN_4O_{11.5}Pb$	$C_{35}H_{44}Cl_2N_4O_{13}Pb$
fw	472.62	795.97	1013.48	1006.83
space group	$P\bar{1}$ (No. 2)	$P\bar{1}$ (No. 2)	$C2/c$ (No. 15)	$P2_1/n$ (No. 14)
a, Å	10.5052(8)	7.9580(2)	40.3616(6)	13.4691(2)
b, Å	11.2181(9)	10.2778(2)	10.5905(1)	17.7452(2)
c, Å	12.8678(9)	11.4938(2)	19.8960(3)	15.8320(2)
α, deg	67.738(2)	68.257(1)		
β, deg	85.477(2)	71.202(1)	100.129(1)	92.509(1)
γ, deg	68.6820(1)	68.324(1)		
V, Å^3	1304.3(2)	792.52(3)	8371.99(19)	3780.41(9)
Z	2	1	8	4
T, K	298(2)	298(2)	298(2)	173(2)
λ, Å (Mo Kα)	0.71073	0.71073	0.71073	0.71073
D_{calcd}, g/cm^3	1.203	1.668	1.608	1.769
μ, mm^{-1}	0.082	5.496	4.159	4.675
R1 ($I > 2\sigma(I)$)[a]	0.0672	0.0418	0.0506	0.0277
wR2 (all data)[a]	0.2055	0.0942	0.1300	0.0653

[a] $R1 = \sum||F_o| - |F_c||/\sum|F_o|$, $wR2 = \{\sum[w(|F_o|^2 - |F_c|^2|)^2]/\sum[w(F_o^4)]\}^{1/2}$.

interested in the relationship between structure and stability of lead(II) complexes with macrocyclic ligands. In a previous work,[14] we have reported a novel family of Schiff-base cryptands (L^4−L^7) containing two different binding units: a rigid and unsaturated N_2X set (X: N, O) and a flexible and cyclic N_2O_n set linked by aromatic bridges. These cryptands structurally derive from bibracchial lariat ethers incorporating pendant aniline moieties, and constitute the first examples of lateral macrobicycles containing imine groups. In a subsequent work,[15] we have carried out studies to assess the different complexation capabilities of the bibracchial lariat ether L^1 and the related lateral macrobicycle L^4 toward lead(II) and cadmium(II). More recently, we have also reported the synthesis of the bibracchial lariat ether L^3 and its metal complexes with Cu(II)[16] and the lanthanide(III) ions.[17]

As a continuation of these works, in the present paper we report the complexation properties of the two lariat ethers *N*,*N*′-bis(2-aminobenzyl)-4,13-diaza-18-crown-6 ($\mathbf{L^2}$) and *N*,*N*′-bis[(2-salicylaldimino)benzyl]-4,13-diaza-18-crown-6 ($\mathbf{L^3}$) and the lateral macrobicycle $\mathbf{L^7}$ toward Pb(II). These macrocyclic receptors have been chosen by the different number and topology of donor atoms arranged along their pendant arms, but maintaining the diaza-18-crown-6 moiety into their backbones. In addition, the presence of either flexible side chains, in $\mathbf{L^2}$ and $\mathbf{L^3}$, or a well-fastened one ($\mathbf{L^7}$) provides them a different grade of rigidity, so allowing a comparative study of the structure and stability of their Pb(II) complexes on the basis of both electronic and steric effects.

Scheme 1

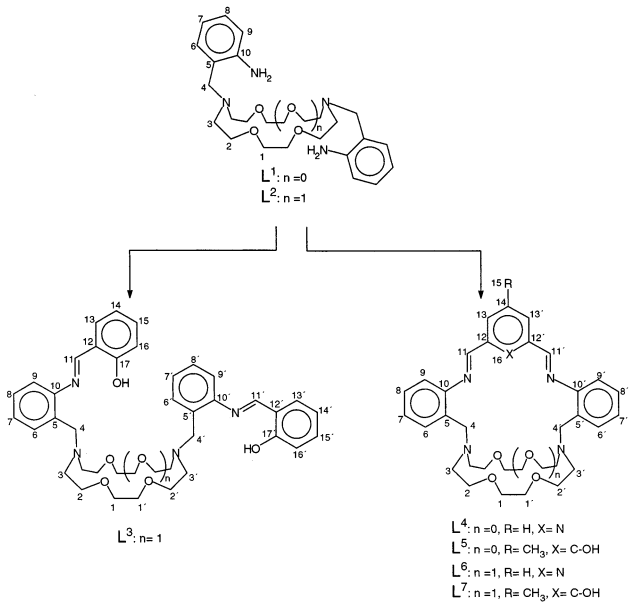

Experimental Section

Materials. 2,6-Diformyl-4-methylphenol was synthesized according to the literature method.[18] *N*,*N*′-Bis-(2-aminobenzyl)-4,13-diaza-18-crown-6 ($\mathbf{L^2}$) and *N*,*N*′-bis(2-salicylaldiminobenzyl)-4,13-diaza-18-crown-6 ($\mathbf{L^3}$) were prepared as we described previously.[16] Recrystallization of $\mathbf{L^2}$ from absolute ethanol/diethyl ether (1:1) gave single crystals suitable for X-ray diffraction. The barium cryptate $[BaL^7](ClO_4)_2 \cdot 2H_2O$ was prepared by a procedure similar to that previously described[14] for the thiocyanate salt (yield: 0.116 g (79%)). Anal. Calcd for $C_{35}H_{44}BaCl_2N_4O_{13} \cdot 2H_2O$: C, 43.2; H, 5.0; N, 5.8. Found: C, 43.7; H, 4.7; N, 5.4. FAB-MS (*m*/*z*): 837 ($[BaL^7(ClO_4)]^+$), 737 ($[BaL^7]^+$). IR (KBr): ν(C═N) 1635, ν(C═C) 1601, 1535, ν_{as}(Cl−O) 1088, δ_{as}(O−Cl−O) 623 cm^{-1}.^{1}H NMR in CD_3CN: δ 16.76 (1H, b, −OH), 8.51 (1H, s, H11), 7.65 (1H, s, H11′), 6.8−7.6 (10H, m), 3.2−4.5 (28H, m), 2.35 (3H, s, H15).

All other chemicals were purchased from commercial sources and used without further purification. Solvents were of reagent grade purified by the usual methods.

(12) Liu, L. K.; Lin, C.-S.; Young, D.-S.; Shyu, W.-J.; Ueng, C.-H. *Chem. Commun.* **1996**, 1255.
(13) Smith, S. V.; Harrowfield, J. M.; Di Bartolo, N. M.; Sargeson, A. M. *PCT Int. Appl.* **2000**.
(14) Esteban, D.; Bañobre, D.; Bastida, R.; de Blas, A.; Macías, A.; Rodríguez, A.; Rodríguez-Blas, T.; Fenton, D. E.; Adams, H.; Mahía, J. *Inorg. Chem.* **1999**, *38*, 1937.
(15) Esteban, D.; Bañobre, D.; de Blas, A.; Rodríguez-Blas, T.; Bastida, R.; Macías, A.; Rodríguez, A.; Fenton, D. E.; Adams, H.; Mahía, J. *Eur. J. Inorg. Chem.* **2000**, 1445.
(16) Rodríguez-Infante, C.; Esteban, D.; Avecilla, F.; de Blas, A.; Rodríguez-Blas, T.; Mahía, J.; Macedo, A. L.; Geraldes, C. F. G. C. *Inorg. Chim. Acta* **2001**, *317*, 190.
(17) Platas, C.; Avecilla, F.; de Blas, A.; Rodríguez-Blas, T.; Bastida, R.; Macías, A.; Rodríguez A.; Adams, H. *J. Chem. Soc., Dalton Trans.* **2001**, 1699.
(18) Taniguchi, S. *Bull. Chem. Soc. Jpn.* **1984**, *57*, 2683.

CAUTION! Although we have experienced no difficulties with the perchlorate salts, these should be regarded as potentially explosive and handled with care.[19]

Preparation of the Complexes. [PbL²](ClO₄)₂ (1). A solution of $Pb(ClO_4)_2 \cdot H_2O$ (0.057 g, 0.135 mmol) in absolute ethanol (40 mL) was added with stirring to a solution of **L²** (0.064 g, 0.135 mmol) in absolute ethanol (20 mL). The reaction mixture was stirred and refluxed for 5 h. During the reaction a white precipitate appeared. It was collected by filtration, washed with absolute ethanol, and air-dried (yield: 0.09 g (76%)). Anal. Calcd for $C_{26}H_{40}Cl_2N_4O_{12}Pb$: C, 35.5; H, 4.5; N, 6.4. Found: C, 35.5; H, 4.6; N, 6.4. FAB-MS (*m*/*z*): 779 ($[PbL^2(ClO_4)]^+$). IR (KBr): $\nu_{as}(NH_2)$ 3334, $\nu_s(NH_2)$ 3270, $\delta(NH_2)$ 1617, ν(C═C) 1585, 1497, $\delta(CH_2)$ 1456, ν_{as}(ClO) 1088, δ_{as}(O−Cl−O) 624 cm^{-1}. Λ_M (acetonitrile): 284 Ω^{-1} cm^2 mol^{-1} (2:1 electrolyte). Solution ^{1}H NMR: Table 3.

[PbL²](SCN)₂·H₂O·EtOH (2a). $Pb(SCN)_2$ (0.034 g, 0.105 mmol) was added to a stirred solution of the ligand **L²** (0.050 g, 0.105 mmol) in absolute ethanol (10 mL). The reaction mixture was stirred and refluxed for 12 h. Upon cooling, a white precipitate appeared, which was collected by filtration, washed with absolute ethanol, and air-dried (yield: 0.061 g (73%)). Anal. Calcd for $C_{28}H_{40}N_6O_4PbS_2 \cdot H_2O \cdot EtOH$: C, 41.9; H, 5.6; N, 9.8. Found: C, 41.7; H, 5.2; N, 9.8. FAB-MS (*m*/*z*): 737 ($[PbL^2(SCN)]^+$), 679 ($[PbL^2]^+$). IR (KBr): $\nu_{as}(NH_2)$ 3283, $\nu_s(NH_2)$ 3243, $\delta(NH_2)$ 1612, ν(C═C) 1585, 1496, $\delta(CH_2)$, 1457, ν(SCN) 2030 cm^{-1}. Λ_M (acetonitrile): 148 Ω^{-1} cm^2 mol^{-1} (1:1 electrolyte). Solution ^{1}H NMR: Table 3. Slow diffusion of diethyl ether into a solution of **2a** in acetone gave single crystals of formula $[PbL^2](SCN)_2$ (**2b**) suitable for X-ray crystallography.

[Pb(L³-H)](ClO₄)·H₂O (3a). The bibracchial lariat ether **L²** (0.050 g, 0.105 mmol) and salicylaldehyde (0.026 g, 0.211 mmol) were dissolved in absolute ethanol (60 mL) and heated to reflux. After 4 h, triethylamine (0.043 g, 0.420 mmol) was added, and the reflux was maintained for 3 h. $Pb(ClO_4)_2 \cdot 6H_2O$ (0.054 g, 0.105 mmol) was then added, and the reflux was maintained for 8 h. The resultant deep yellow solution was filtered while hot and the filtrate rotary-evaporated to 20 mL. Upon cooling to room temperature, a yellow precipitate was formed and collected by filtration (yield: 0.060 g (58%)). Anal. Calcd for $C_{40}H_{47}ClN_4O_{10}Pb \cdot H_2O$: C, 48.7; H, 4.8; N, 5.6. Found: C, 48.3; H, 4.6; N, 5.4. FAB-MS (*m*/*z*): 887 ($[Pb(L^3\text{-}H)]^+$). IR (KBr): ν(C═N) 1611, ν(C═C) 1578, 1533, 1483, $\delta(CH_2)$ 1456, ν_{as}(ClO) 1095, δ_{as}(O−Cl−O) 624 cm^{-1}. Λ_M (acetonitrile): 126 Ω^{-1} cm^2 mol^{-1} (1:1 electrolyte). X-ray quality crystals of formula $[Pb(L^3\text{-}H)](ClO_4) \cdot 1.5H_2O$ **(3b)** were grown by slow evaporation of a methanolic solution of **3a**.

[Pb(L³-H)](SCN)·H₂O (4). The yellow complex was prepared as described for **3a** by using $Pb(SCN)_2$ (0.034 g, 0.105 mmol) (yield: 0.055 g (55%)). Anal. Calcd for $C_{41}H_{47}N_5O_6PbS \cdot H_2O$: C, 51.1; H, 5.1; N, 7.3. Found: C, 51.0; H, 5.2; N, 7.2. FAB-MS (*m*/*z*): 887 ($[Pb(L^3\text{-}H)]^+$). IR (KBr): ν(C═N) 1610, ν(C═C) 1577, 1532, 1481, $\delta(CH_2)$ 1456, ν(SCN) 2055 cm^{-1}. Λ_M (acetonitrile): 137 Ω^{-1} cm^2 mol^{-1} (1:1 electrolyte).

[PbL⁷](ClO₄)₂·2.5H₂O. Method 1 (5a). The bibracchial lariat ether **L²** (0.036 g; 0.076 mmol) and $Pb(ClO_4)_2 \cdot 3H_2O$ (0.050 g; 0.117 mmol) were dissolved in absolute ethanol (35 mL). The mixture was vigorously stirred and heated while a solution of 2,6-diformyl-4-methylphenol (0.012 g; 0.076 mmol) in 50 mL of absolute ethanol was added dropwise. After the addition was complete, the resulting solution was stirred and refluxed for 5 days. The orange solution was filtered while hot and cooled to room temperature. The orange precipitate formed was collected by filtration (yield: 0.025 g (31%)). Anal. Calcd for $C_{35}H_{44}Cl_2N_4O_{13}Pb \cdot 2.5H_2O$: C, 39.95; H, 4.6; N, 5.3. Found: C, 39.9; H, 4.4; N, 5.2. FAB-MS (*m*/*z*): 907

(19) Wolsey, W. C. *J. Chem. Educ.* **1973**, *50*, A335.

Table 2. Selected Bond Lengths (Å) and Angles (deg) for **L²** and Complexes **2**, **3**, and **5**

L² [a]

N(1)−C(1)	1.375(4)	N(4)−C(26)	1.378(3)
N(2)−C(7)	1.462(4)	N(3)−C(17)	1.476(3)
N(2)−C(8)	1.472(3)	N(3)−C(19)	1.474(3)
N(2)−C(11)	1.472(3)	N(3)−C(20)	1.472(3)
O(1)−C(9)	1.418(3)	O(3)−C(15)	1.413(3)
O(1)−C(10)	1.378(3)	O(3)−C(16)	1.413(3)
O(2)−C(12)	1.415(4)	O(4)−C(14A)	1.402(3)
O(2)−C(13)	1.335(4)	O(4)−C(18)	1.415(3)
N(1)−C(1)−C(2)	120.2(2)	N(4)−C(26)−C(21)	119.7(2)
N(1)−C(1)−C(6)	120.7(2)	N(4)−C(26)−C(25)	121.2(2)
N(2)−C(7)−C(6)	115.8(2)	N(3)−C(19)−C(18)	115.7(2)
N(2)−C(8)−C(9)	111.3(2)	N(3)−C(17)−C(16)	111.7(2)
C(10)−O(1)−C(9)	113.5(2)	C(15)−O(3)−C(16)	113.9(2)
C(13)−O(2)−C(12)	118.0(3)	C(18)−O(4)−C(14A)	114.6(2)
C(7)−N(2)−C(8)	109.4(2)	C(17)−N(3)−C(20)	109.6(2)
C(7)−N(2)−C(11)	110.3(2)	C(17)−N(3)−C(19)	112.3(2)
C(8)−N(2)−C(11)	113.4(2)	C(20)−N(3)−C(19)	109.2(2)

2b [b]

Pb(1)−O(1)	2.638(4)	Pb(1)−N(1)	2.683(4)
Pb(1)−O(2)	2.686(5)	Pb(1)−N(2)	2.795(4)
O(1)−Pb(1)−O(2)	61.6(2)	O(1)−Pb(1)−O(2A)	118.41(16)
O(1)−Pb(1)−N(2)	65.7(1)	O(1)−Pb(1)−N(2A)	114.3(1)
O(2)−Pb(1)−N(2)	114.8(1)	O(2)−Pb(1)−N(2A)	65.2(1)
N(1)−Pb(1)−O(1)	93.6(1)	N(1)−Pb(1)−O(1A)	86.4(1)
N(1)−Pb(1)−O(2)	74.2(1)	N(1)−Pb(1)−O(2A)	105.8(1)
N(1)−Pb(1)−N(2)	73.7(1)	N(1)−Pb(1)−N(2A)	106.3(1)

3b

Pb(1)−O(1)	2.304(5)	Pb(1)−N(1)	2.493(5)
Pb(1)−N(3)	2.665(5)	Pb(1)−O(2)	2.675(4)
Pb(1)−O(4)	2.791(4)	Pb(1)−O(5)	2.801(4)
Pb(1)−O(3)	2.855(5)	Pb(1)−N(4)	2.982(5)
O(1)−Pb(1)−N(1)	73.8(2)	O(1)−Pb(1)−N(3)	98.4(2)
N(1)−Pb(1)−N(3)	74.3(2)	O(1)−Pb(1)−O(2)	76.5(2)
N(1)−Pb(1)−O(2)	124.3(2)	N(3)−Pb(1)−O(2)	64.7(2)
O(1)−Pb(1)−O(4)	159.7(2)	N(1)−Pb(1)−O(4)	91.1(2)
N(3)−Pb(1)−O(4)	63.8(2)	O(2)−Pb(1)−O(4)	102.3(1)
O(1)−Pb(1)−O(5)	126.2(1)	N(1)−Pb(1)−O(5)	72.2(2)
N(3)−Pb(1)−O(5)	110.8(2)	O(2)−Pb(1)−O(5)	156.9(1)
O(4)−Pb(1)−O(5)	58.4(1)	O(1)−Pb(1)−O(3)	86.6(2)
N(1)−Pb(1)−O(3)	157.5(2)	N(3)−Pb(1)−O(3)	120.5(2)
O(2)−Pb(1)−O(3)	59.1(2)	O(4)−Pb(1)−O(3)	110.4(2)
O(5)−Pb(1)−O(3)	112.9(1)	O(1)−Pb(1)−N(4)	88.1(2)
N(1)−Pb(1)−N(4)	105.6(2)	N(3)−Pb(1)−N(4)	173.1(2)
O(2)−Pb(1)−N(4)	119.4(2)	O(2)−Pb(1)−N(4)	119.4(2)
O(4)−Pb(1)−N(4)	109.4(1)	O(5)−Pb(1)−N(4)	63.1(1)
O(3)−Pb(1)−N(4)	61.8(1)		

5b

Pb(1)−O(1)	2.351(2)	Pb(1)−N(1)	2.548(2)
Pb(1)−O(4)	2.553(2)	Pb(1)−O(2)	2.573(2)
Pb(1)−N(3)	2.712(2)	Pb(1)−O(3)	2.734(2)
Pb(1)−O(5)	2.941(2)		
O(1)−Pb(1)−N(1)	71.40(6)	O(1)−Pb(1)−O(4)	87.29(6)
N(1)−Pb(1)−O(4)	97.45(7)	O(1)−Pb(1)−O(2)	138.85(6)
N(1)−Pb(1)−O(2)	82.29(6)	O(4)−Pb(1)−O(2)	127.99(5)
O(1)−Pb(1)−N(3)	131.44(6)	N(1)−Pb(1)−N(3)	72.53(6)
O(4)−Pb(1)−N(3)	66.42(6)	O(2)−Pb(1)−N(3)	64.06(6)
O(1)−Pb(1)−O(3)	85.36(6)	N(1)−Pb(1)−O(3)	90.51(6)
O(4)−Pb(1)−O(3)	166.86(6)	O(2)−Pb(1)−O(3)	63.33(5)
N(3)−Pb(1)−O(3)	126.28(6)	O(1)−Pb(1)−O(5)	75.59(6)
N(1)−Pb(1)−O(5)	141.33(6)	O(4)−Pb(1)−O(5)	61.04(6)
O(2)−Pb(1)−O(5)	136.37(5)	N(3)−Pb(1)−O(5)	118.58(6)
O(3)−Pb(1)−O(5)	106.46(5)		

[a] Symmetry transformations used to generate equivalent atoms: A $-x+1, -y+1, -z$. [b] Symmetry transformations used to generate equivalent atoms: A $-x+2, -y, -z+2$.

([PbL^7(ClO$_4$)]$^+$), 807 [PbL^7]$^+$. IR (KBr): ν(C=N) 1635, ν(C=C) 1587, 1558, ν_{as}(Cl−O) 1091, δ_{as}(O−Cl−O) 623 cm^{-1}. Λ_M (acetonitrile): 264 Ω^{-1} cm^2 mol^{-1} (2:1 electrolyte). Solution ^{1}H and ^{13}C NMR: Table 4. Recrystallization of **5a** from acetonitrile gave single crystals of formula [PbL^7](ClO$_4$)$_2$ (**5b**) suitable for X-ray crystallography.

Method 2 (5c). The lead(II) complex of L^7 can be also prepared by transmetalation of the Ba(II) derivative: [BaL^7](ClO$_4$)$_2$·2H$_2$O (0.0177 g; 0.0182 mmol) and 0.0083 g of Pb(ClO$_4$)$_2$·3H$_2$O (0.0182 mmol) were dissolved in hot absolute ethanol (10 mL), and the resultant solution was refluxed with stirring for 48 h. The orange precipitate formed after cooling to room temperature was collected by filtration (yield: 0.0066 g (35%)). Anal. Calcd for C$_{35}$H$_{44}$Cl$_2$N$_4$O$_{13}$Pb·H$_2$O: C, 41.0; H, 4.5; N, 5.5. Found: C, 40.5; H, 4.2; N, 5.2.

Physical Measurements. Elemental analyses and FAB-MS spectra were carried out by Servicios Xerais de Apoio á Investigación of the Universidade da Coruña: elemental analyses were carried out on a Carlo Erba 1180 elemental analyzer, and FAB-MS spectra were recorded on a FISONS QUATRO mass spectrometer with a Cs ion gun using 3-nitrobenzyl alcohol as matrix. ^{1}H and ^{13}C NMR spectra were run on a Bruker AC 200 F or a Bruker WM-500 spectrometer. IR spectra were recorded, as KBr disks, using a Bruker Vector 22 spectrophotometer. Conductivity measurements were carried out at 20 °C with a Crison Micro CM 2201 conductivimeter using 10^{-3} M solutions of the complexes in acetonitrile. Electrospray mass spectra (ES-MS) were obtained in positive mode with a Hewlett-Packard LC-MSD 1100 mass spectrograph from 10^{-4} M acetonitrile solutions by infusion at 0.3 mL/min.

Electronic spectra were recorded at 20 °C on a Perkin-Elmer Lambda 900 UV−vis or Uvikon 942 Plus spectrophotometers using 1.0 cm quartz cells. Spectrophotometric titrations were performed in the latter spectrometer connected to an external computer. Typically, a solution of the ligand (**L^2** or **L^3**) or the Ba(II) complex in acetonitrile (25 or 50 mL) was prepared, and then 25−300 μL aliquots of a solution of Pb(ClO$_4$)$_2$·3H$_2$O ($\sim 10^{-3}$ M) in the same solvent were successively added. The concentrations of the solutions were 1.69×10^{-5} (**L^2**), 1.06×10^{-5} (**L^3-2H**), and 9.44×10^{-6} M (**BaL^7**). The ionic strength was adjusted to $I = 10^{-3}$ M with tetrabutylammonium perchlorate for each titration. For the spectrophotometric titration of **L^3** 2 equiv of Et$_3$N per mol of ligand was used to deprotonate the phenol group. Plots of molar absorption coefficient as a function of the metal:ligand ratio gave a first indication of the number and stoichiometry of the complexes formed in solution in every titration; factor analysis[20] was then applied to the data to confirm the number of absorbing species. Eventually, a model for the distribution of species was fitted with a nonlinear least-squares algorithm to give stability constants using the computer program SPECFIT.[21]

X-ray Crystal Structure Determinations. Three-dimensional X-ray data were collected on a Bruker SMART 1000 CCD diffractometer by the $\phi-\omega$ scan method. Data for **L^2**, **2b**, and **3b** were collected at room temperature, whereas for **5b** it was done at 173 K. Reflections were measured from a hemisphere of data collected of frames each covering 0.3° in ω. Data with 2θ greater than 50° were omitted for **L^2**. Of the 6789, 5575, 27930, and 35284 reflections measured for ligand **L^2** and complexes **2b**, **3b**, and **5b**, all of which were corrected for Lorentz and polarization effects and for absorption by semiempirical methods based on symmetry-equivalent and repeated reflections, 3291, 3751, 5982, and 11463 independent reflections exceeded the significance level $|F|/\sigma(|F|) > 4.0$, respectively. Complex scattering factors were taken from the program package SHELXTL.[22] The structures were solved by direct methods for **L^2**, **2b**, and **5b** and by the Patterson method for **3b** and refined by full-matrix least-squares methods on F^2. The hydrogen atoms were included in calculated positions and refined by using a riding mode, except the hydrogen atoms H1A, H1B, H4A, and H4B for **L^2** and the hydrogen atom H2A for **5b**, which were left to refine freely. Hydrogen atoms of solvent (water molecules) for **3b** were not included. Refinement converged with allowance for thermal anisotropy of all non-hydrogen atoms in all compounds. The crystal of **3b** presents a disorder on the ionic perchlorate, and 32 restraints had to be imposed. This disorder has been resolved, and two atomic sites for the chlorine atom and two oxygen atoms have been observed. The site occupancy factors were 0.500 for Cl(1) and Cl(2), 0.485 for O(9) and O(10), and 0.515 for O(11) and O(12). Minimum and maximum final electron density: −0.257 and 0.494 e Å^{-3} for **L^2**, −2.511 and 1.414 e Å^{-3} (next to the Pb1) for **2b**, −1.424 and 2.044 e Å^{-3} (next to the Pb1) for **3b,** and −1.598 and 1.700 e Å^{-3} (next to the Pb1) for **5b**. Crystal data and details on data collection and refinement are summarized in Table 1.

Results and Discussion

Complexes of L^2. The reaction of the bibracchial lariat ether *N*,*N*′-bis(2-aminobenzyl)-4,13-diaza-18-crown-6 (**L^2**) with lead(II) salts (perchlorate or thiocyanate) in absolute ethanol yielded the colorless complexes [PbL^2](ClO$_4$)$_2$ (**1**) and [PbL^2](SCN)$_2$·H$_2$O·EtOH (**2a**). The IR spectra (KBr disks), display bands at 3334 and 3270 cm^{-1} for **1** and at 3283 and 3243 cm^{-1} for **2a**, corresponding to the ν_{as}(NH$_2$) and ν_s(NH$_2$) stretching modes of the coordinated amine groups, respectively. Bands corresponding to the ν_{as}(ClO) stretching and δ_{as}(OClO) bending modes of the perchlorate groups present in **1** appear without splitting at 1088 and 624 cm^{-1}, respectively, as befits an uncoordinated anion. The IR spectrum of **2** exhibits the thiocyanate stretch at 2030 cm^{-1}.

The structure of the free ligand **L^2** was determined by X-ray diffraction. The **L^2** molecule lies across a crystallographic inversion center, and the asymmetric unit comprises two half-molecules. The structures of both molecules are shown in Figure 1, and selected bond lengths and angles are given in Table 2. The bond lengths and angles do not show any significant deviation from the expected values. Both arms are arranged on opposite sides with respect to the crown moiety, resulting in an anti conformation with distances between both pivotal nitrogen atoms in each of the two L^2 molecules of 8.241 and 7.778 Å. The crystalline packing comes determined by intermolecular hydrogen bonds that imply one proton of the amine group and an oxygen atom of the neighbor molecule. Likewise, it could be stated that strong intramolecular hydrogen bonds exist between −NH$_2$ groups and pivotal nitrogen atoms due to the short N(pivotal)···HN(amine), 2.38(4) and 2.35(3) Å,

(20) Malinowski, E. R.; Howery, D. G. *Factor Analysis in Chemistry*; J. Wiley: New York, Chichester, Brisbane, and Toronto, 1980.
(21) Gampp, H.; Maeder, M.; Meyer, C. J.; Zuberbühler, A. D. *Talanta* **1986**, *33*, 943.
(22) Sheldrick, G. M. *SHELXTL: An Integrated System for Solving and Refining Crystal Structures from Diffraction Data (Revision 5.1)*; Universty of Göttingen: Göttingen, Germany, 1997.

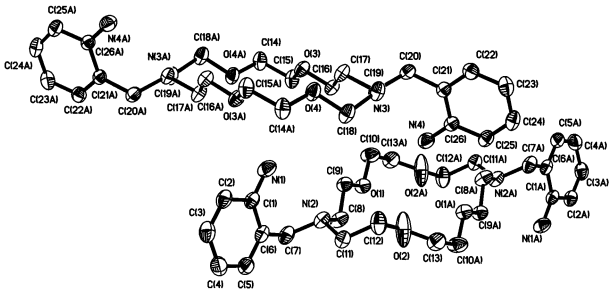

Figure 1. View of the two molecules present in crystals of $\mathbf{L^2}$. Hydrogen atoms are omitted for clarity. The ORTEP plot is at the 30% probability level.

and N(amine)···N(pivotal), 3.003(4) and 3.073(3) Å, distances.[23]

Crystals **2b** contain the cation $[PbL^2]^{2+}$ and two thiocyanate anions involved in hydrogen bond interactions with the $-NH_2$ groups, as it follows from the N(1)···N(1S) distances (3.243(7) and 3.078(7) Å) and from the N(1)−H(1A)−N(1S) and N(1)−H(1B)−N(1S) angles (175.4° and 177.2°, respectively). Figure 2a displays a view of the complex cation. It contains a PbN_4O_4 core with the eight heteroatoms of $\mathbf{L^2}$ coordinated to the lead(II) ion. All the bond lengths, compiled in Table 2 together with bond angles of the coordination sphere, fall within the range reported for the previously described[15] [Pb(*N*,*N*′-bis(2-aminobenzyl)-1,10-diaza-15-crown-5)]$^{2+}$; but, unlike this one, in $[PbL^2]^{2+}$ the metal ion lies on a center of symmetry. The organic receptor $\mathbf{L^2}$ adopts an anti arrangement in **2b**, although the presence of the lead(II) ion in its cavity causes important structural changes, particularly in the fold of the crown and arms, as can be appreciated by comparing Figures 1 and 2. This is confirmed by comparing the distances between donor atoms that give an idea about the size of the macrocyclic cavity: in **2b**, the distance between both aniline donors [N(1)−N(1A)] amounts to 5.367 Å (12.918 and 12.508 Å in $\mathbf{L^2}$), whereas the distance between both pivotal nitrogen atoms [N(2)−N(2A)] is 5.590 Å (8.241 and 7.778 Å in $\mathbf{L^2}$). This evidences the flexibility of this receptor, which feels largely the presence of a Pb(II) ion lodged into its cavity. So, whereas the conformation of the free ligand $\mathbf{L^2}$ is governed by the hydrogen bond N(amine)···N(pivotal), in complex **2b** this receptor $\mathbf{L^2}$ adopts a conformation leading to get the maximum interaction with the lead(II) guest, which results in a coordination polyhedron around the Pb(II) ion that can be described as a slightly distorted cube formed by the eight donor atoms of the receptor (Figure 2b), with mean deviation from planarity of the six square faces of the polyhedron ranging from 0.1849 to 0.1061 Å. The cubic coordination occurs very infrequently in discrete complexes because a distortion of the polyhedron toward a square antiprism or a triangulated dodecahedron alleviates the repulsion between the donor atom of the ligand(s) maintaining the M−X distances, and in $[PbL^2]^{2+}$ is probably due to the balance of flexibility and rigidity in the crown moiety and in the pendant arms of $\mathbf{L^2}$.

(23) Desiraju, G. R.; Steiner, T. *The Weak Hydrogen Bond*; Oxford University Press: Oxford, 1999.

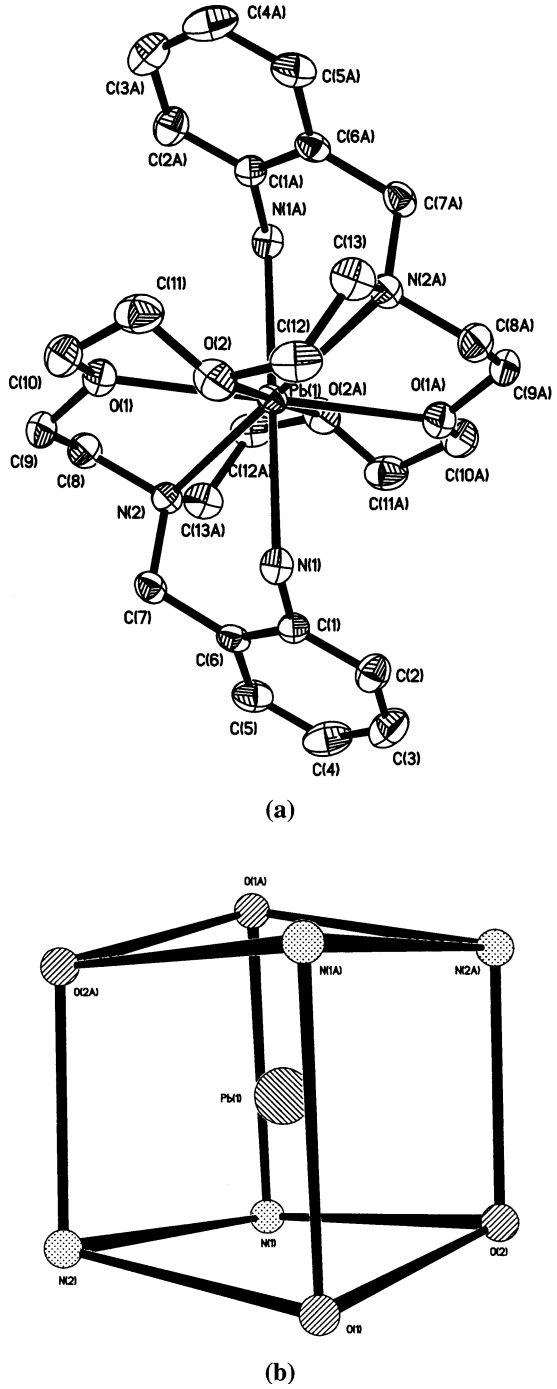

Figure 2. X-ray crystal structure of complex $[PbL^2]^{2+}$ showing the atomic numbering scheme. Hydrogen atoms are omitted for clarity. The ORTEP plot is at the 30% probability level.

The behavior in acetonitrile-d_3 solution of complexes **1** and **2a** was investigated by ^{1}H NMR spectroscopy in the temperature range 228−348 K (see Scheme 1 for labeling scheme). At 348 K, the ^{1}H NMR spectrum of **1** displays only four resonances of aliphatic protons, in agreement with an effective C_{2h} symmetry in solution (as expected from the solid state structure): H1 and H4 appear as the expected singlets, whereas H2 and H3 appear as triplets (Figure 3). Upon coordination to Pb(II) the signals of $\mathbf{L^2}$ corresponding to protons H2, H3, and H4 shift downfield by 0.36−0.28 ppm whereas the signal corresponding to H1 shifts up-

Table 3. Proton NMR Data (ppm) for $\mathbf{L^2}$ and the Complexes **1** and **2a**

	NH_2	H1	H3	H2	H4	H6	H8	H7	H9
$L^{2\,a}$	4.97(s), 4H	3.49(s), 8H	2.64(t), 8H	3.54(t), 8H	3.54(s), 4H	6.96(d), 2H	7.02(t), 2H	←6.57(m), 4H→	
1[b]	4.64(br), 4H	3.31(br), 8H	2.98(dd), 8H	3.83(br), 8H	3.91(s), 4H	←7.32(m), 4H→		←7.03(m), 4H→	
2[c]	4.57(s), 4H	3.40(s), 8H	2.96(dd), 8H	3.82(dd), 8H	3.89(s), 4H	←7.26(m), 4H→		←6.97(m), 4H→	

[a] Conditions: Assignment supported by 2D H,H COSY, HMQC, and HMBC experiments at 293 K, CD_3CN, 500 MHz. $J_{23} = J_{32} = 5.33$ Hz, $J_{67} = J_{76} = 7.07$ Hz. Chemical shifts (without assignment) of the different multiplets for H2, H4, H7, and H9 are given only. [b] Conditions: $T = 308$ K, CD_3CN, 200 MHz. Coupling constants determined for a A_2B_2 system: $J_{2a3a} = J_{3a2a} = J_{2b3a} = J_{3a2b} = 5.38$ Hz, $J_{2b3b} = J_{3b2b} = J_{2a3b} = J_{3b2a} = 4.88$ Hz. ^{1}H NMR of **1** at 348 K displays H1 as a singlet and H2 as a double-doublet (dd) for an A_2B_2 system. Coupling constants determined: $J_{2a3a} = J_{3a2a} = J_{2b3a} = J_{3a2b} = 5.37$ Hz, $J_{2b3b} = J_{3b2b} = J_{2a3b} = J_{3b2a} = 4.88$ Hz. Chemical shifts (without assignment) of the different multiplets for aromatic protons are given only. [c] Conditions: $T = 308$ K, CD_3CN, 200 MHz. Coupling constants determined for a A_2B_2 system: $J_{2a3a} = J_{3a2a} = J_{2b3a} = J_{3a2b} = 5.37$ Hz, $J_{2b3b} = J_{3b2b} = J_{2a3b} = J_{3b2a} = 4.89$ Hz. Chemical shifts (without assignment) of the different multiplets for aromatic protons are given only.

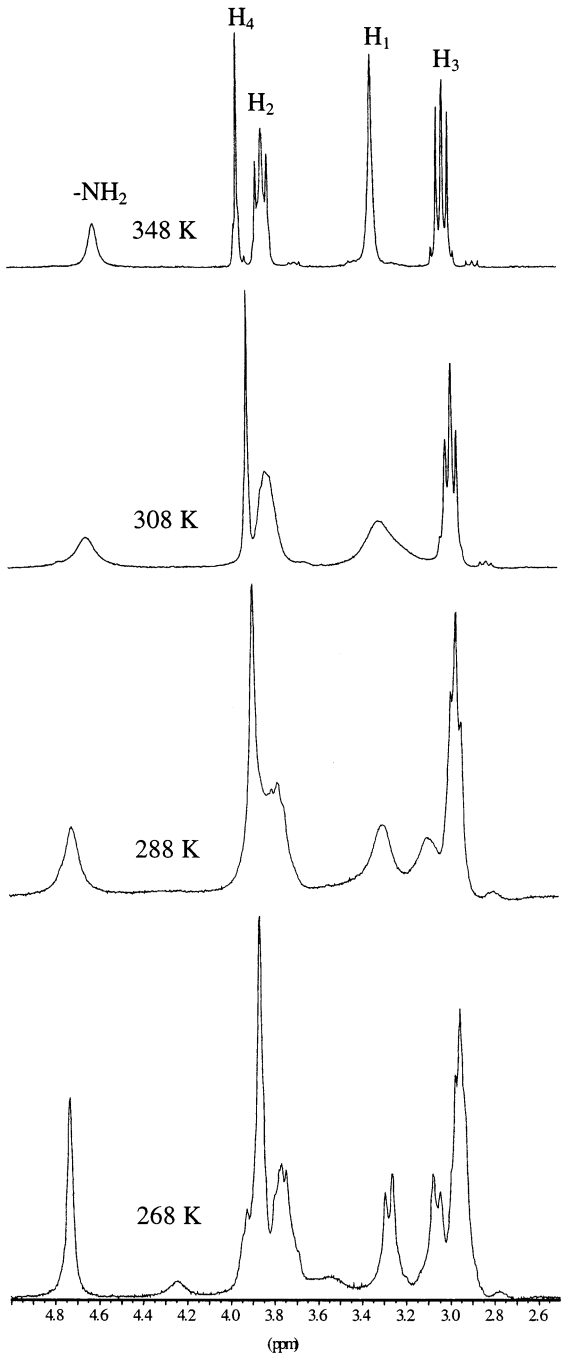

Figure 3. Part of the 200 MHz ^{1}H NMR spectra of **1** recorded in acetonitrile-d_3 at different temperatures.

field by 0.17 ppm (Table 3). Signals corresponding to the aromatic rings are shifted downfield whereas the singlet signal of amine protons is shifted upfield by 0.40 ppm as a consequence of the coordination of the amine groups to the Pb(II) ion. Upon decreasing the temperature the signals corresponding to the H1−H4 protons gradually broaden, reflecting intramolecular conformational exchange processes (Figure 3). In spite of the increasing complexity of the spectra on decreasing the temperature, some temperature dependent spectral changes can be analyzed and interpreted. At 268 K, the signals of the geminal H1 protons ($H1_{axial}$ and $H1_{equatorial}$) appear as an AB spin system with a coupling constant of 6.35 Hz. These resonances gradually broaden above this temperature, and finally they coalesce at ca. 308 K, reflecting intramolecular conformational exchange processes that correspond to a $\delta \leftrightarrow \lambda$ conformational interconversion in the five-membered chelate ring formed by the metal-bound moiety.[24] From the coalescence temperature of the diasterotopic signals $H1_{axial}$ and $H1_{equatorial}$, we can estimate an activation barrier of $\Delta G^{\ddagger} = 66 \pm 5$ kJ mol^{-1} for this intramolecular dynamic process. Similar intramolecular dynamic processes are probably responsible for the broadening of the signals corresponding to the H2 and H3 protons below 348 K, but a detailed line shape analysis and a determination of $\Delta G^{\ddagger}$ has not been possible due to overlaps with other signals.

The ^{1}H spectrum of **2a** in acetonitrile-d_3 at 348 K is nearly identical to that of **1**, and decreasing the temperature also results on a gradual broadening of the proton signals. At 248 K, two pairs of signals are observed for the H1 ($H1_{axial}$ and $H1_{equatorial}$) and H3 protons ($H3_{axial}$ and $H3_{equatorial}$). Both pairs of signals coalesce at a temperature close to 268 K, which allows the estimation of the activation barrier for the $\delta \leftrightarrow \lambda$ conformational exchange of both chelate rings $\overline{\text{M−O−C−C−O}}$ and $\overline{\text{M−O−C−C−N}}$: $\Delta G^{\ddagger} = 57 \pm 2$ and 58 ± 2 kJ mol^{-1}, respectively. These values are ~10 kJ mol^{-1} smaller than the one determined for **1**. This suggests that the counterion affects the dynamic behavior of the $\mathbf{L^2}$ complexes in acetonitrile solution, rendering the five-membered chelate rings formed by the metal-bound moieties more rigid in **1** than in **2a**. Moreover, conductivity measurements carried out in acetonitrile solution show that **2a** ($\Lambda_M = 148\ \Omega^{-1}$ cm^2 mol^{-1}) behaves as a 1:1 electrolyte and **1** ($284\ \Omega^{-1}$ cm^2 mol^{-1}) behaves as a 2:1 electrolyte,[25] suggesting that the presence of a coordinated thiocyanate group affects the $\delta \leftrightarrow \lambda$ conformational exchange. This points to

(24) Schlager, O.; Wieghardt, K.; Grondey, H.; Rufinska, A.; Nuber, B. *Inorg. Chem.* **1995**, *34*, 6440.

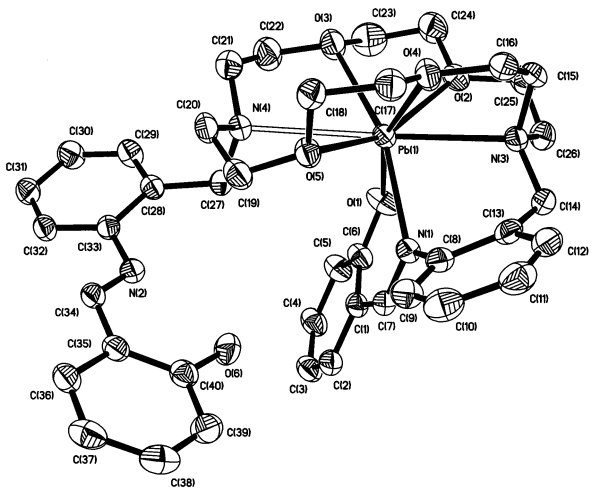

Figure 4. X-ray crystal structure of complex $[Pb(L^3\text{-}H)]^+$ showing the atomic numbering scheme. Hydrogen atoms are omitted for clarity. The ORTEP plot is at the 30% probability level. Hollow bonds indicate weak Pb−X interactions.

the structure of **2a** in acetonitrile solution being different from that found for **2b** in the solid state, the latter showing two uncoordinated thiocyanate groups. Further cooling below 268 K reveals that the signals due to the $H1_{axial}$ and $H1_{equatorial}$ protons in complex **1** broaden again, reflecting a new intramolecular conformational exchange process. This would also explain the fact that $\delta(1) \neq {}^1/_2[\delta(H1_{axial}) + \delta(H1_{equatorial})]$ in the temperature range 348−368 K. We also observe that, when the temperature decreases below 288 K, the signal due to the amine protons broadens in complex **1**, and finally it splits into two different resonances, which points to the presence of two different isomers of complex **1** in acetonitrile solution (Figure 3), the interconversion process between the two isomers probably being responsible for this second dynamic process in solution.

Complexes of L^3. Reaction of *N*,*N*′-bis(2-aminobenzyl)-4,13-diaza-18-crown-6 ($\mathbf{L^2}$) and salicylaldehyde in the presence of triethylamine and a lead(II) salt (perchlorate or thiocyanate) under the conditions described in the Experimental Section gave the analytically pure products $[Pb(L^3\text{-}H)](ClO_4)\cdot H_2O$ (**3a**) and $[Pb(L^3\text{-}H)](SCN)\cdot H_2O$ (**4**), respectively. The presence of an intense absorption at ca. 1610 cm^{-1}, attributable to the $\nu(C{=}N)_{imine}$ stretching mode in both infrared spectra (KBr disks), together with the absence of carbonyl and amine bands, confirms the Schiff base formation in situ. This band appears at 1618 cm^{-1} in the spectrum of the uncoordinated lariat ether $\mathbf{L^3}$,[16] and it is slightly shifted to lower wavenumbers by deprotonation and complexation. Likewise, the IR spectrum of **3a** also displays bands at 1095 and 624 cm^{-1} corresponding to the asymmetric stretching and bending modes of the perchlorate groups. These bands appear clearly without splitting, as befits an uncoordinated anion. The IR spectrum of **4** features an intense band at 2055 cm^{-1} due to the ν(CN) stretching mode of the thiocyanate group.

Crystals of **3b** contain the cation $[Pb(L^3\text{-}H)]^+$, a well-separated perchlorate anion, and water molecules. Figure 4 displays a view of the structure of the cation, and selected bond lengths and angles are given in Table 2. The incorporation of a salicylic fragment in each side arm of the parent macrocycle *N*,*N*′-bis(2-aminobenzyl)-4,13-diaza-18-crown-6 ($\mathbf{L^2}$) leads to a coordination environment around lead(II) ion and a conformation of the organic receptor in $[Pb(L^3\text{-}H)]^+$ different from that found for $[PbL^2]^{2+}$ in **2b**. Figure 4 shows how the metal ion is pushed out from the crown hole, the bibracchial lariat ether presents a syn arrangement, and one of the arms remains uncoordinated. The phenol and imine group of this arm are involved in hydrogen-bonding interaction [O(6)···N(2) 2.592(7) Å; O(6)H(6)···N(2) 1.86 Å; O(6)−H(6)−N(2) 147.7°]. The lead(II) ion is now seven-coordinated, bound to the phenolate oxygen, O(1), and the imine nitrogen atom, N(1), of one side arm, one of the pivotal nitrogen atoms, N(3), and the four oxygen atoms of the crown, O(2)−O(5). These last four Pb−O distances range from 2.675(4) to 2.855(5) Å, and they are slightly longer than the sum of the van der Waals radius of oxygen and the ionic radius of lead(II) of 2.67 Å.[26,27] The distance between the lead(II) ion and the pivotal nitrogen atom N(4) is 2.982-(5) Å, considerably longer than the unequivocal Pb−N bonds. This distance is 0.317 Å longer than the distance to the opposite donor atom N(3) [Pb−N(3) 2.665(5) Å]. The question is whether it is due to an active lone pair on the lead(II) atom or not. It has been suggested that the presence of a stereochemically active lone pair on Pb(II) will result in a concomitant shortening of the Pb(II)−X bond on the side of the lead(II) away from the site of the stereochemically active lone pair.[28−30] In these so-called hemi-directed compounds, the difference between Pb(II)−X and Pb(II)−*lp*-X (the latter being the distance between Pb(II) and a ligand X in the direction of the lone pair, opposite to the Pb(II)−X direction) has been found to range from 0.3 to 1.2 Å.[30] Likewise, it has been reported that in compounds where the lone pair is active, the Pb−N bond lengths fall into the range 2.37−2.56 Å, whereas for an inactive lone pair, the Pb−N bond lengths fall in the range 2.62−2.88 Å.[28] According to all of this, our structure would be in the limit of a hemi-directed ligand distribution, and the asymmetrical disposition of the lead(II) ion in this structure could be due not only to sterical features but also to the active lone pair on the lead-(II) ion. Hemi-directed ligand distribution is usually found for lead(II) compounds having coordination numbers 2−5; however, lead(II) compounds having coordination numbers 6−8 can also exhibit hemi direction, particularly when hard oxygen and/or nitrogen donor atoms are available.[30]

In $[Pb(L^3\text{-}H)]^+$ the crown moiety is folded in pseudo-boat conformation and only N(4), O(3), O(4), and O(5) are essentially coplanar (rms deviation from planarity 0.0384 Å),

(25) Geary, W. J. *Coord. Chem. Rev.* **1971**, *7*, 81.
(26) Ahrens, L. H. *Geochim. Cosmochim. Acta* **1952**, *2*, 155.
(27) Pauling, L. *The Nature of the Chemical Bond*, 3rd ed.; Cornell University Press: Ithaca, NY, 1960.
(28) Hancock, R. D.; Shaikjee, M. S.; Dobson, S. M.; Boeyens, J. C. A. *Inorg. Chim. Acta* **1988**, *154*, 229.
(29) Hancock, R. D. In *Perspectives in Coordination Chemistry*; Williams, A. F., Floriani, C., Merbach, A. E., Eds.; Verlag HCA: Weinheim, 1992.
(30) Shimoni-Livny, L.; Glusker, J. P.; Bock, C. W. *Inorg. Chem.* **1998**, *37*, 1853.

the Pb(II) being located 1.4298 Å beneath the plane. The distances between both imine nitrogen atoms and between both pivotal nitrogen atoms are 5.622 and 5.637 Å, respectively, the latter being slightly longer than that found in **2b**.

The ^{1}H NMR spectra of complexes **3a** and **4** run in CD_3CN solution at room temperature are virtually identical, suggesting that the nature of the counterion does not affect the structure of the complexes in solution. At room temperature, the ^{1}H NMR spectrum features two signals for the imine protons [δ 8.53(s, 1H)), 8.38(s, 1H))], the latter ascribed to the coordinated imine group and the former to the uncoordinated one, as well as the signal of the phenol proton of the noncoordinated pendant arm at δ 12.67 (1H). This suggests that these complexes adopt a similar conformation in solution and in the solid state, in which one pendant arm remains uncoordinated. Asymmetric coordination of the lead(II) ion gives rise to the appearance of complicated multiplets in the aromatic region as well as overlapped broad signals in the region below $\delta = 4$, which prevented a full assignment of the spectra. At 268 K and 200 MHz the imine proton signal shows satellites attributable to proton coupling to the naturally abundant ^{207}Pb ($I = {}^1/_2$),[31] reflecting kinetic inertness in the complexes as well as a degree of covalence in the interaction with the nearby donor atom. So, the signal at δ 8.38 appears as a singlet flanked by the satellites, with a ^3J(H$-^{207}$Pb) of 17.09 Hz. This coupling value reflects a very strong interaction between the Pb(II) ion and the coordinated imine nitrogen atom in these compounds, confirmed by the short Pb−N(imine) distance found in the solid state [Pb−N(1) 2.493(5) Å]. For instance, a ^3J(H$-^{207}$Pb) of 2.93 Hz has been reported for a Pb(II) complex with a related macrobicyclic receptor for which a much longer Pb−N(imine) bond distance was found in the solid state (2.74 Å).[15]

Complexes of L^7. Reaction of equimolar amounts of 2,6-diformyl-4-methylphenol and *N*,*N*′-bis(2-aminobenzyl)-4,13-diaza-18-crown-6 (**L^2**) in the presence of lead(II) perchlorate in absolute ethanol, as described in the Experimental Section, gave the analytically pure orange product [PbL^7](ClO$_4$)$_2$·2.5H$_2$O (**5a**) in 31% yield. The IR and FAB-mass spectra confirmed that condensation and [1 + 1] cyclization had occurred and the lead(II) complex was formed. Together with bands at 1091 and 623 cm^{-1} assigned to the asymmetric stretching and bending modes of the perchlorate groups, the IR spectrum (KBr disks) of **5a** also features a band at 1635 cm^{-1} attributable to a ν(C=N)$_{imine}$ stretching mode, but no bands due to amine or carbonyl vibration modes. The FAB-mass spectrum, obtained using 3-nitrobenzyl alcohol as the matrix, displays peaks at *m*/*z* (% BPI) = 907 (16), 807 (73), and 601 (100) due to [PbL^7(ClO$_4$)]$^+$, [PbL^7]$^+$, and [L^7 + H]$^+$, respectively. Compound **5a** can also be prepared by a transmetalation reaction using the corresponding barium complex, [BaL^7](ClO$_4$)$_2$·2H$_2$O, and lead(II) perchlorate. Reaction in a 1:1 molar ratio in absolute ethanol gave **5a** in 35% yield. The absence of peaks corresponding to species containing the BaL^7 fragment in the FAB-mass spectrum coupled with the presence of peaks due to [PbL^7(ClO$_4$)]$^+$, [PbL^7]$^+$, and [L^7 + H]$^+$ confirmed that the transmetalation reaction occurred and the macrobicycle **L^7** remained intact in the lead(II) complex.

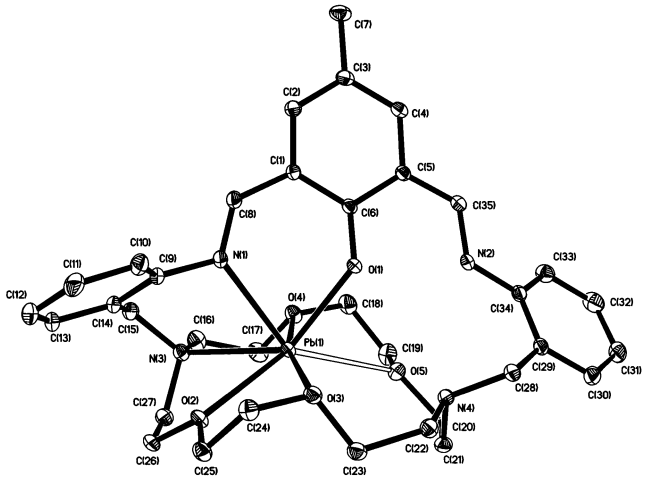

Figure 5. X-ray crystal structure of complex [PbL^7]$^{2+}$ showing the atomic numbering scheme. Hydrogen atoms are omitted for clarity. The ORTEP plot is at the 30% probability level. Hollow bonds indicate weak Pb−X interactions.

Crystals **5b** consist of the [PbL^7]$^{2+}$ cation (Figure 5) and two well-separated perchlorate groups. Table 2 summarizes bond lengths and angles. The lead(II) ion is asymmetrically placed at one end of the macrobicyclic cavity coordinated to one imine nitrogen atom, N(1), one pivotal nitrogen atom, N(3), the phenolate oxygen atom, O(1), and three oxygen atoms of the crown moiety, O(2), O(3), and O(4). The considerably long distance Pb−O(5) of 2.941(2) Å suggests a very weak interaction of the lead(II) ion with O(5). Likewise, the lead(II) ion is clearly closer to O(2) and O(4) [Pb−O(2) 2.573(2) Å, Pb−O(4) 2.553(2) Å] than to O(3) [Pb−O(3) 2.734(2) Å]. The other two heteroatoms of the macrobicyclic receptor, the imine and pivotal nitrogen atoms N(2) and N(4), do not form a part of the lead(II) coordination environment, as evidenced by the observed Pb−N(2) and Pb−N(4) distances of 4.349 and 3.612 Å, respectively. The presence of a relatively rigid third chain in the structure of the receptor causes a different folding of the crown moiety compared to the one observed in **3**, where the lead(II) ion is also asymmetrically coordinated to the receptor. Both pivotal nitrogen atoms [N(3), N(4)] and the oxygen donors [O(5), O(3)] are essentially coplanar (rms deviation from planarity 0.0113 Å), with the oxygen O(2) located 0.9606 Å above the plane and the lead(II) ion and the oxygen O(4) lying 0.4783 and 0.9496 Å, respectively, beneath it. The distance between both imine nitrogen atoms is 5.417 Å, whereas both pivotal nitrogen atoms are separated 6.230 Å, the latter distance again being longer than those found in **2b** and **3b**. The X-ray data suggest that proton transfer from phenol to imine N has occurred [N(2)−H(2A) 0.80(3) Å, O(1)−H(2A) 1.93(3) Å]. The imine nitrogen N(2) and the phenol oxygen atom O(1) are involved in hydrogen-bonding interaction [O(1)···N(2) 2.567(3) Å; O(1)···H(2A)N(2) 1.93(3) Å; O(1)−H(2A)−N(2) 137(3)°], as well as N(2) and the uncoordinated pivotal nitrogen atom N(4) [N(2)···N(4) 3.183(3) Å;

(31) Bashall, A.; McPartlin, M.; Murphy, B. P.; Powell, H. R.; Waikar, S. *J. Chem. Soc., Dalton Trans.* **1994**, 1283.

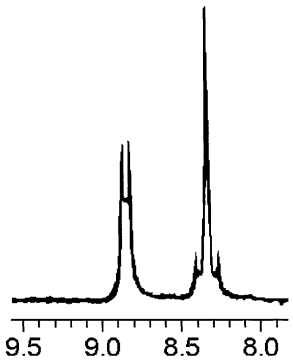

Figure 6. Part of the ^{1}H NMR spectrum of **5** showing ^{207}Pb satellites (ppm).

N(2)H(2A)···N(4) 2.65(3) Å; N(2)−H(2A)−N(4) 125(2)°], although the latter is considerably weaker than the former.

The ^{1}H and ^{13}C NMR spectra of **5a** recorded in CD_3CN (Table 4) indicate that this asymmetric structure is also maintained in solution. Assignments were achieved with the aid of 2D H,H COSY and HMQC experiments and substituent shift calculations (Figures 4S and 5S, Supporting Information). In the ^{1}H NMR spectrum, again the signals corresponding to the ethylene protons of the crown moiety appear at high field as complicated overlapping multiplets, their unequivocal assignment being impossible. The signal at δ 8.43 due to the imine proton H11 appears as a singlet flanked by the satellites attributable to proton coupling to ^{207}Pb, with a ^3J(H−^{207}Pb) of 21.00 Hz (see Figure 6), as also observed for compounds **3a** and **4**. This coupling value again reflects a very strong interaction between the Pb(II) ion and the imine nitrogen N(1), and consequently, a large degree of covalence in this interaction, which also agrees with the short distance Pb−N(1), 2.548(2) Å, found in the X-ray crystal structure. The signal corresponding to the other imine proton, H11′ (δ 8.77), appears as a doublet (J = 12.62 Hz) (Figure 6), suggesting the proton transfer from the phenol to the uncoordinated imine nitrogen N(2) (in agreement with the solid state data), as observed previously for lead(II) imino−phenol cryptates in solution.[32]

Spectrophotometric Titrations. UV−vis spectroscopy is a general method used for the assessment of the coordination environment and to determine the stability constants of metal complexes, but it has been less exploited, compared with potentiometric methods, for the study of macrocyclic metal complexes.[33] The presence of benzo groups in the ligand backbone increases the absorption coefficients rendering the absorbance useful for the spectrophotometric studies. The UV−vis spectrum of the free ligand $\mathbf{L^2}$, recorded in acetonitrile solution, features two absorption bands with maxima at 236 and 288 nm corresponding to E_2 and B charge-transfer bands of the aromatic rings, respectively.[34] After complexation to Pb(II), the absorption appearing at lower energies exhibits a blue shift due to the coordination of the amine groups, thus enabling the formation of the complexes in solution to be monitored.

Table 4. Proton and Carbon-13 NMR Data[a] Corresponding to $\mathbf{L^7}$ for the Complex **5a**

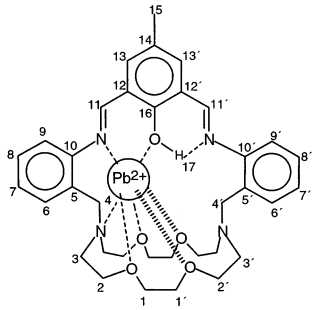

proton	δ	carbon-13	δ
H17	15.46 (1H, br)		
		C16	170.2
H11′	8.77 (1H, d)[b]	C11′	162.8
H11	8.43 (1H, s)[c]	C11	168.7
H13′	7.79 (1H, s)	C13′	142.4
H13	7.77 (1H, s)	C13	148.7
H8, H8′, H7′	7.61 (3H, m)	C8, C8′, C7	130.8, 129.9, 121.4
H6, H6′, H9′	7.48 (3H, d)	C6, C6′, C9′	131.6, 131.4, 129.6
H7	7.38 (1H, t)	C7′	127.3
H9	7.11 (1H, d)[d]	C9	123.5
		C5, C5′, C12, C12′, C14	131.1, 125.8, 125.5, 126.0, 118.1
H1, H1′, H2, H2′, H4, H4′	2.5−3.5 [e]	C1, C2, C3, C3′, C4, C4′	69.8, 68.5, 61.5, 61.3, 58.1, 57.4
H3, H3′	2.5−3.5 [e]		
H15	2.37 (3H, s)	C15	18.6

[a] Values in ppm relative to $SiMe_4$ at 293 K, 500 MHz, CD_3CN as solvent. [b] $J_{11',NH17}$ = 12.62 Hz. [c] Metal satellite observed corresponding to coupling to ^{207}Pb, $J_{11,^{207}Pb}$ = 21.00 Hz. [d] $J_{9,8}$ = 7.27 Hz. [e] Chemical shift (without assignment) of the different multiplets for crown protons are given only.

The electronic absorption spectrum of $\mathbf{L^3}$ in acetonitrile solution displays a maximum at 334 nm attributable to the imine chromophore[12] and two more intense bands at 262 and 229 nm. Deprotonation of $\mathbf{L^3}$ with triethylamine does not modify the spectrum, except for the intensity of the high-energy band, which increases after addition of the base. Spectrophotometric investigation of the deprotonation of $\mathbf{L^3}$ with Et_3N in acetonitrile revealed two inflection points near the Et_3N:L^3 ratios 1 and 2, which would imply the successive formation of the $\mathbf{(L^3\text{-}H)^-}$ and $\mathbf{(L^3\text{-}2H)^{2-}}$ species. However, the analysis of the data to estimate the successive equilibrium constants did not converge properly due to the small changes observed in the spectra upon addition of the base. After complexation of Pb(II) to $\mathbf{(L^3\text{-}2H)^{2-}}$ the three $\pi \rightarrow \pi^*$ transitions undergo a red shift, and a new band appears centered at 388 nm, which was used to monitor the formation of the complex in solution. This band is attributed to a metal-perturbed charge-transfer transition within the coordinated imine group.[35]

The spectrophotometric titrations of $\mathbf{L^2}$ (1.69×10^{-5} M) and $\mathbf{(L^3\text{-}2H)^{2-}}$ (1.06×10^{-5} M) with $Pb(ClO_4)_2 \cdot 3H_2O$ were performed in acetonitrile over Pb(II):L molar ratios 0−2.4 $\mathbf{(L^2)}$ and 0−6 $\mathbf{(L^3\text{-}2H)^{2-}}$. Two equivalents of Et_3N per mol

(32) Drew, M. G. B.; Howarth, O. W.; Morgan, G. G.; Nelson, J. *J. Chem. Soc., Dalton Trans.* **1994**, 3149.
(33) Izzat, R. M.; Pawlak, K.; Bradshaw, J. S. *Chem. Rev.* **1995**, *95*, 2529.
(34) Silverstein, R. M.; Bassler, C. *Spectrometric Identification of Organic Compounds*; Wiley Int.: New York, 1967.
(35) Bashall, A.; McPartlin, M.; Murphy, B. P.; Powell, H. R.; Waikar, S. *J. Chem. Soc., Dalton Trans.* **1994**, 1383.

of $\mathbf{L^3}$ were added to ensure the complete deprotonation of the ligand. The data displayed a single inflection point when the Pb:ligand molar ratio is close to 1 for both titrations, indicating the existence of only one complex species in solution; factor analysis was then applied to the data to confirm the number of absorbing species. The spectrophotometric titrations were satisfactorily fitted with the equilibriums 1 and 2, allowing the estimation of the stability constants in acetonitrile solution, which amount to log $K[PbL^2] = 7.7 \pm 0.5$ and log $K[Pb(L^3\text{-}2H)] = 7.2 \pm 0.2$.

$$Pb^{2+} + L^2 \leftrightarrow [Pb(L^2)]^{2+} \quad (1)$$

$$Pb^{2+} + (L^3\text{-}2H)^{2-} \leftrightarrow [Pb(L^3\text{-}2H)] \quad (2)$$

The ligand $\mathbf{L^7}$ can only be synthesized by a metal template procedure, i.e., by using Ba(II) or Pb(II) as template ions. These ions remain coordinated inside the cavity of $\mathbf{L^7}$, which prevents the estimation of stability constants of $\mathbf{L^7}$ with other metal ions by direct methods. However, spectrophotometric titrations of $[BaL^7](ClO_4)_2$ with Pb(II) can provide some information about the number of species in solution during the transmetalation process, and also about its stoichiometry and stability. The importance of these studies lies in the fact that many transition and post-transition metal complexes with Schiff-base ligands are generally obtained by transmetalation reactions from the corresponding Ba(II), Sr(II), or Ca(II) complexes.[36] The spectrophotometric titration of $[BaL^7](ClO_4)_2$ (9.56×10^{-4} M) with $Pb(ClO_4)_2 \cdot 3H_2O$ was performed in acetonitrile over Pb(II):L molar ratios 0−4.8. The subsequent data displayed inflection points near the Pb:$[BaL^7]^{2+}$ molar ratios 0.5, 1, and 1.5, which would imply the existence of at least three Pb(II) complex species in solution. This result was confirmed by factor analysis,[20] and the spectrophotometric data were satisfactorily fitted with the equilibriums 3, 4, and 5, allowing an estimation of the overall equilibrium constants $\log(\beta_{12}^{Pb}) = 11.9 \pm 0.2$, $\log(\beta_{11}^{Pb}) = 6.1 \pm 0.3$, and $\log(\beta_{32}^{Pb}) = 24.2 \pm 0.2$. A distribution diagram of the different species formed in solution during the transmetalation process is given in Figure 8S (Supporting Information).

$$Pb^{2+} + 2[BaL^7]^{2+} \leftrightarrow [Pb(BaL^7)_2]^{6+} \qquad \log(\beta_{12}^{Pb}) \quad (3)$$

$$Pb^{2+} + [BaL^7]^{2+} \leftrightarrow [Pb(L^7)]^{2+} + Ba^{2+} \qquad \log(\beta_{11}^{Pb}) \quad (4)$$

$$Pb^{2+} + 2[PbL^7]^{2+} \leftrightarrow [Pb_3(L^7)_2]^{6+} \qquad \log(\beta_{32}^{Pb}) \quad (5)$$

The use of electrospray mass spectrometry (ES-MS) to characterize qualitatively the distribution of preformed ions in solution has been well documented.[37] Solutions of $[BaL^7](ClO_4)_2$ and Pb(II) with a total Ba(II) concentration of 10^{-3} M were prepared with the following stoichiometric Pb:Ba ratios: 1:2, 4:5, 1:1, 6:5, 3:2, and 2:1. At low Pb(II) concentration (1:2 Pb/Ba) the spectra display peaks assigned to the protonated free ligand $[L^7 + H]^+$ ($m/z = 601.3$) and the $[BaL^7]^{2+}$ cation. The spectrum also displays a very intense peak due to the $[Pb(BaL^7)_2(ClO_4)_2]^{4+}$ species ($m/z = 473.3$). When the Pb:Ba ratio is increased, new peaks due to the $[PbL^7(ClO_4)]^+$ ($m/z = 907.3$) and $[PbL^7]^+$ ($m/z = 808.0$) appear, as well as a less intense peak at $m/z = 709.1$ attributable to the $[Pb_3(L^7)_2(ClO_4)_3]^{3+}$ cation. These data qualitatively confirm the speciation established by the spectrophotometric study and therefore the formation of polynuclear species during the transmetalation process.

Conclusions

The bibracchial lariat ether *N*,*N*′-bis(2-aminobenzyl)-4,13-diaza-18-crown-6 ($\mathbf{L^2}$) can be easily functionalized by reaction of its amine groups with salicylaldehyde or 2,6-diformyl-4-methylphenol to yield a family of ligands which form stable complexes with lead(II) salts. The different denticity and grade of rigidity of these receptors from $\mathbf{L^2}$ to $\mathbf{L^7}$ is reflected in the different coordination environment found for the lead(II) ion in the corresponding complexes. So, in the solid state, with the most flexible receptor $\mathbf{L^2}$ the lead(II) ion is eight-coordinated and fits quite well into the crown hole favoring an anti arrangement of the organic receptor, the counterions being out of the coordination sphere. The coordination polyhedron around the Pb(II) ion can be described as a distorted cube, which occurs very infrequently in discrete complexes, and in this case probably arises from the adequate balance of flexibility and rigidity in the crown moiety and in the pendant arms of $\mathbf{L^2}$.

Condensation of a salicylic fragment with each side arm of $\mathbf{L^2}$ gives $\mathbf{L^3}$, which forms cationic complexes of formula $[Pb(L^3\text{-}H)]^+$. Independent of the different nature of the counterion present (thiocyanate or perchlorate), in this complex the metal ion is asymmetrically placed into the receptor cavity and only seven-coordinated being pushed out of the crown hole; the organic receptor presents a syn arrangement, and one of its arms remains uncoordinated. The lead(II) ion is also asymmetrically placed into the cavity of the third macrocycle ($\mathbf{L^7}$), a lateral macrobicycle incorporating a well-fastened phenolyl Schiff-base spacer. Steric requirements seem to be responsible for this asymmetric disposition of the metal ion in these compounds, although the active lone pair on the lead(II) atom could be also responsible for this feature in compound **3b**. Likewise, we have also found that the flexible crown moiety adopts very different conformations in the lead(II) complexes of $\mathbf{L^2}$, $\mathbf{(L^3\text{-}H)^-}$, and $\mathbf{L^7}$, which allows the lead(II) ion to fit into the cavity of ligands with a different number and topology of donor atoms and side chains with different rigidity.

Spectrophotometric titrations recorded in acetonitrile solution demonstrate that the stability of the Pb(II) complexes with $\mathbf{L^2}$ and $\mathbf{(L^3\text{-}2H)^{2-}}$ is very similar. This is probably because, first, increasing the number of donor atoms available for the coordination to Pb(II) does not result on an increase of the coordination number around Pb(II) since one of the pendant arms of $\mathbf{(L^3\text{-}H)^-}$ remains uncoordinated both in the solid state and in solution and, second, the coordination of Pb(II) to the very rigid negatively charged arm of $\mathbf{(L^3\text{-}H)^-}$ "pulls" the metal ion out of the cavity of the macrocycle.

(36) Collinson, S. R.; Fenton, D. E. *Coord. Chem. Rev.* **1996**, *148*, 19.
(37) Martin, N.; Bünzli, J.-C. G.; Mckee, V.; Piguet, C.; Hopfgartner, G. *Inorg. Chem.* **1998**, *37*, 577.

The lead complexes discussed in this paper open the way for the design of an entire class of new compounds by, for instance, reduction of the imine groups. This would increase the flexibility of the macrocyclic cavity, which may favor a more efficient encapsulation of lead(II) and/or other metal ions.

Acknowledgment. The authors thank Professor L. Fabbrizzi (Università di Pavia, Italy) for his facilities to perform the stability constant determinations and Xunta de Galicia (PGIDT00MAM10302PR) for generous financial support. D.E. also thanks Xunta de Galicia for a research grant.

Supporting Information Available: X-ray crystallographic files in CIF format for $\mathbf{L^2}$, **2**, **3**, and **5**, Figures 1S−5S (showing 2D H,H COSY, HMQC, and HMBC experiments), and Figure 6S (showing distribution diagrams obtained from spectrophotometric titrations). This material is available free of charge via the Internet at http://pubs.acs.org.

IC0255095